Bulletin of the JSME Vol.9, No.3, 2015
Journal of Advanced Mechanical Design, Systems, and Manufacturing

On the analysis of double wishbone suspension

Engin TANIK* and Volkan PARLAKTAŞ*
*Department of Mechanical Engineering,
Hacettepe University, Beytepe, Çankaya, 06800 Ankara, Turkey
E-mail: volkan@hacettepe.edu.tr

Received 2 June 2015

Abstract
This paper introduces novel approaches for analysis of the double wishbone suspension mechanism. In the literature, to the best of our knowledge there is no analysis study available for the double wishbone mechanism that is performed "analytically". Initially kinematic model of the double wishbone mechanism is established. Then, a kinematic analysis methodology is presented. This analysis procedure is carried out analytically. The essential parameters; camber, caster, kingpin, toe angles, and track variation are defined according to the kinematic model. A double wishbone suspension mechanism is synthesized as an example by using the method presented in this study. Variations of the essential parameters with respect to wheel travel are plotted. The synthesized mechanism is established both in Lotus Suspension Analysis and Catia software and same results with the analytical model are obtained. Thus, it is verified that mechanisms of different dimensions can be analyzed and parameters can be optimized precisely and swiftly by using this analytical approach.

Key words : Suspension systems, Double wishbone, RSSR-SS mechanism, Suspension linkage, Suspension kinematics

1. Introduction

The purpose of a vehicle suspension is to maximize the contact between tires and road surface for good road holding, to provide steering stability for good handling and to ensure comfort of passengers for good ride. Vehicles' road holding and handling performance mainly depend on the kinematic characteristics of vehicle suspension systems. From a kinematics point of view, a suspension system can be defined as a combination of links and joints. Changes in orientation and positions undergone by wheel during bump and rebound are called the kinematic characteristics defined by means of some functional parameters, whose values are specified by the design. A higher performance in the design is achieved as kinematic characteristics are improved. The most important kinematic parameters of suspension systems that effect handling, road holding, and ride characteristics are camber, caster, kingpin, and toe angle (Reimpell and Stoll, 1998). Coordinates of hard points and/or lengths of linkages are commonly considered as design variables to optimize performance of suspension systems. Due to the complexity of suspension systems, models are usually developed by using some commercial software.

Independent suspension is a broad term for any vehicle suspension system that allows each wheel on the same axle to move independently of each other. Independent suspension typically offers better ride quality and handling characteristics, due to lower unsprung weight and ability of each wheel to address road undisturbed by activities of other wheel on vehicles. The existence of different topologies and configurations confirms that there is no unique solution adapting well to all situations (Raghavan, 1991). The Macpherson strut (Habibi, et al., 2008) is a popular choice due to its simplicity and low manufacturing cost, but the design has a few disadvantages. Kinematic analysis shows it can't allow vertical movement of the wheel without some degree of either camber angle change. It is not generally considered to give as good handling as a double wishbone suspension, because it allows the engineers less freedom in design. A double wishbone suspension is an independent suspension design using two wishbone-shaped arms to locate wheel. This type of suspension system is also known as the acronym SLA (short-long arm) due to its

Paper No.15-00297
[DOI: 10.1299/jamdsm.2015jamdsm0037]

unequal length of arms. A double wishbone suspension is basically a spatial four-mechanism (Russell, et al., 2009). Each wishbone is connected by two revolute joints to the chassis and by one spherical joint to the knuckle. Shock absorber and coil spring mount to the wishbones to control vertical movement. In the case of front axle, steering knuckle is connected to chassis by means of tie-rod using spherical joints as seen in Fig. 1. Rear suspensions may contain a similar link, called control linkage. Thus, due to this configuration, the whole three-dimensional kinematic chain is named RSSR–SSP (R: revolute, S: spherical, P: prismatic). Large number of design parameters necessary to define a double-wishbone suspension system makes it easy to approach the kinematic characteristic accurately, but at the same time, it is more difficult to synthesize due to the large number of parameters involved in the three-dimensional problem. Double wishbone designs allow the engineer to carefully control the motion of the wheel throughout suspension travel, controlling such parameters as camber angle, caster angle, toe pattern, roll center height and more. The disadvantage is that it is slightly more complex than other systems like a MacPherson strut. Double wishbones are usually considered to have superior dynamic characteristics and are still available on higher performance vehicles.

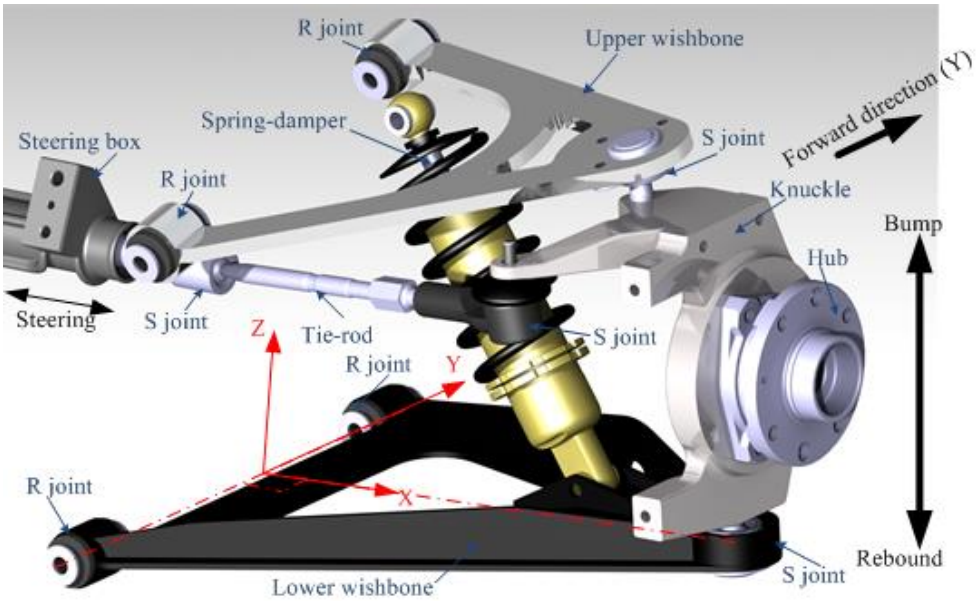

Fig. 1. Double wishbone suspension system

Kinematic design of double-wishbone suspension system using a multi objective dimensional synthesis technique is focused (Sancibrian, et al., 2010). A new design optimization framework for suspension systems considering the kinematic characteristics, such as the camber angle, caster angle, kingpin inclination angle, and toe angle in the presence of uncertainties is proposed (Wu, et al., 2014) . A general method of the kinematic synthesis of suspension mechanisms is presented (Suh, 1989). Design and implementation of a double wishbone front suspension for a vineyard–orchard tractor is dealed (Uberti, et al., 2015). Kinematic design methodology of a suspension system using axiomatic design is presented (Bae, et al., 2002). Dynamic analysis of the double wishbone automotive suspension system using the point-joint coordinates formulation is presented (Attia, 2002). Two position synthesis method is applied to obtain desired camber variation of an approximated double-wishbone mechanism (Tanık and Parlaktas, 2015). Formulation of a comprehensive kineto-dynamic quarter-car model to study the kinematic and dynamic properties of a linkage suspension, and influences of linkage geometry on selected performance measures is presented (Balike, et al., 2011).

In the literature, to the best of our knowledge there is no analysis study available for the double wishbone mechanism that is performed “analytically”. In most foundations such suspension systems are analyzed via high cost software that are based on numerical methods (e.g. Lotus suspension analysis programmer). In this study, we presented a novel kinematic analysis procedure for double wishbone suspension mechanism based on analytical methods. The proposed analytical model can be used precisely for the kinematic design and analysis of double wishbone mechanisms instead of commercial software. In this study, initially kinematic model of the double wishbone suspension mechanism is established. Then, an analysis procedure of the double wishbone mechanism is proposed. The kinematic parameters; camber, caster, kingpin, toe angles and track variation are defined according to the model. In the design example, a

[DOI: 10.1299/jamdsm.2015jamdsm0037]

specific mechanism is analyzed and the kinematic parameters determined from the analytical model are plotted with respect to wheel travel. The same mechanism is analyzed by two different commercial software and the results are compared. With this study, camber, caster, kingpin (steering axis inclination), toe, and track variation with respect to wheel travel of the double wishbone mechanism can be analyzed.

2. Kinematic model of the double wishbone suspension mechanism

A double wishbone suspension is essentially an RSSR–SSP linkage when steering is variable as shown in Fig. 2, and it is RSSR–SS (Shen, et al., 2014) when steering is fixed at a specific position. RSSR-SSP mechanism is constituted by rigidly connecting an SSP linkage; *DEF*, to the RSSR linkage; *OABC*. When P joint is fixed to a specific position, RSSR-SS linkage can be analyzed with the proposed analytical model in this study. DOF (degree-of-freedom) of the RSSR-SSP mechanism is three. However, one of these freedoms, which is the rotation of the tie rod with respect to its own axis (*FE* line), is redundant. Therefore, effective DOF of the mechanism is two, where one is assigned to steering and the other to suspension travel. Since steering box of vehicles is located transversely and symmetrically, steering input is towards X-axis as seen in Fig. 2. Rotation axis of the lower wishbone is on the direction of motion of vehicle which is assigned as Y-axis. Rotation axis of the upper wishbone can be defined with two structure angles: ξ and ϕ. Here, ϕ is the anti-dive (or lift) angle, ξ is yaw angle of the upper wishbone. According to Fig. 2, l_l: length of lower wishbone (*OA*), l_u: length of upper wishbone (*BC*), l_k: length of knuckle (*AB*), t_r: length of tie-rod or control linkage (*FE*), s_a: steering arm length (*ED*), l_{hub}: length of hub (*GW*), l_a: |*AD*|, l_h: |*AH*|, c_o: caster offset |*HG*|, l_{hubt}: |*HW*|, $\vec{e}_i$: unit vector on i^{th} link, R_w: effective radius of the tire (*WJ*), ϕ: anti-dive angle, ξ: yaw angle, θ: lower wishbone angle measured counter-clockwise, χ: angular displacement of upper wishbone measured counter clockwise (Tanık and Parlaktas, 2011, 2015).

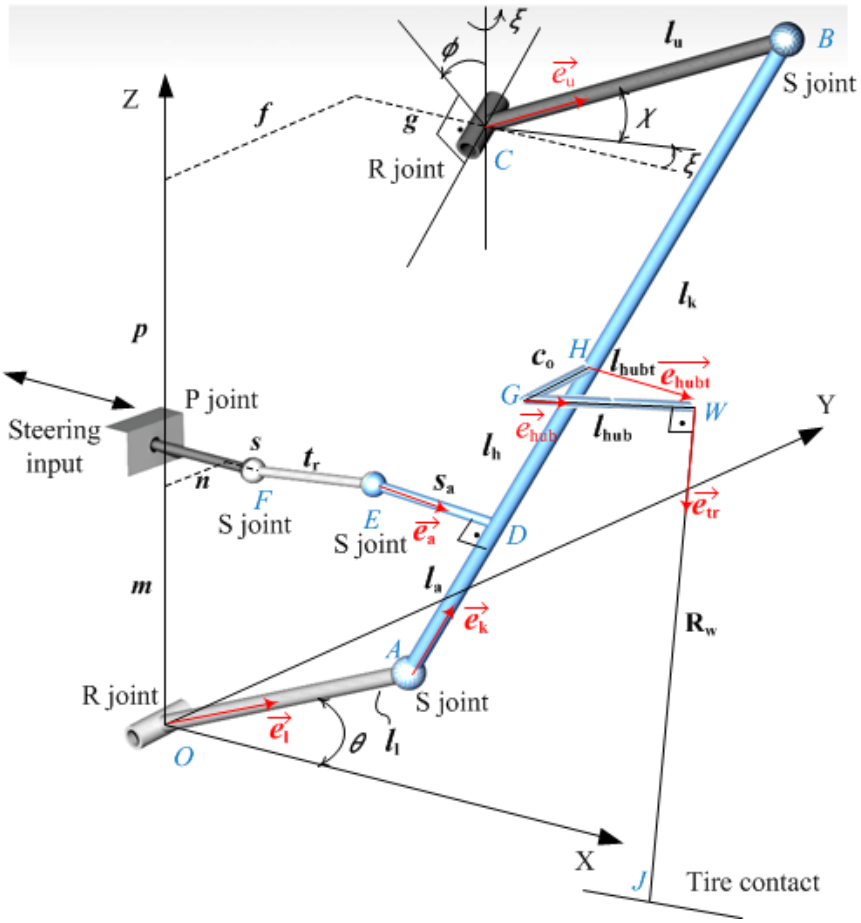

Fig. 2. Kinematic model of the double-wishbone suspension mechanism

[DOI: 10.1299/jamdsm.2015jamdsm0037]

3. Analysis of the double wishbone mechanism

Since a double wishbone mechanism is formed by RSSR and SSP linkages, the complete kinematic analysis can be performed with two independent loops which are *OABCO* and *OADEFO* (Fig.2). Initially, loop of the RSSR linkage; *OABCO* is taken into consideration. It should be noted that, the position of ball joint at F is considered to be fixed at a specific position. In order to perform the analysis of RSSR linkage, the required structure parameters are: l_l, l_u, l_k, ξ and ϕ. When these parameters are specified, RSSR linkage can be analyzed for a given set of lower wishbone angle θ as follows. Vector equation for this loop is: $|\overrightarrow{AB}| = |\overrightarrow{OB} - \overrightarrow{OA}|$. Vectors on the right hand side can be written as:

$$|\overrightarrow{OA}| = l_l \cos\theta \vec{\imath} + l_l \sin\theta \vec{k} \tag{1}$$

$$|\overrightarrow{OB}| = (g + l_u \cos\chi\cos\xi + l_u \sin\chi \sin\phi \sin\xi)\vec{\imath} + (f + l_u \cos\chi \sin\xi - l_u \sin\chi \sin\phi \cos\xi)\vec{\jmath} + (p + l_u \sin\chi \cos\phi)\vec{k} \tag{2}$$

General displacement equation of the RSSR linkage can be obtained as:

$$k_1 + (k_2 - k_3 \cos\theta)\cos\chi - (k_4 + k_5 \sin\theta - k_6 \cos\theta)\sin\chi - k_7 \cos\theta - k_8 \sin\theta = 0 \tag{3}$$

where

$k_1 = f^2 + g^2 + p^2 + {l_l}^2 + {l_u}^2 - {l_k}^2$, $k_2 = 2f l_u \sin\xi + 2g l_u \cos\xi$, $k_3 = 2l_l l_u \cos\xi$, $k_5 = 2l_l l_u \cos\phi$

$k_4 = 2f l_u \cos\xi \sin\phi - 2p l_u \cos\phi - 2g l_u \sin\xi \sin\phi$, $k_6 = 2l_l l_u \sin\xi \sin\phi$, $k_7 = 2g l_l$, $k_8 = 2p l_l$

For a given set of lower wishbone angle θ, values of χ can be determined from Eq. (3) by applying the half tangent formula:

$$\chi = 2\tan^{-1}\left(\frac{-B \pm \sqrt{B^2 - 4AC}}{2A}\right) \tag{4}$$

where

$A = -k_1 + k_2 - k_3 \cos\theta + k_7 \cos\theta + k_8 \sin\theta$

$B = 2k_4 + 2k_5 \sin\theta + 2k_6 \cos\theta$

$C = -k_1 - k_2 - k_3 \cos\theta + k_7 \cos\theta + k_8 \sin\theta$

The position vector of the knuckle can be defined as: $\overrightarrow{AB} = l_k \overrightarrow{e_k}$, where unit vector of the knuckle is determined as:

$$\overrightarrow{e_k} = \frac{1}{l_k}\begin{bmatrix} g + l_u \cos\chi\cos\xi + l_u \sin\chi \sin\phi \sin\xi - l_l \cos\theta \\ f + l_u \cos\chi \sin\xi - l_u \sin\chi \sin\phi \cos\xi \\ p + l_u \sin\chi \cos\phi - l_l \sin\theta \end{bmatrix} \tag{5}$$

Unit vector of the lower wishbone can be defined as:

$$\overrightarrow{e_l} = [\cos\theta \quad 0 \quad \sin\theta]^T \tag{6}$$

By using Eqns. (4-6) one can determine positions of the wishbones and knuckle for a given set of θ in closed-form equation set.

Now, the loop of the SSP linkage; *OADEFO* is taken into consideration to complete the analysis. For this analysis,

[DOI: 10.1299/jamdsm.2015jamdsm0037]

the required structure parameters are: initial coordinates of ball joints E and F (note that F is fixed to a specific position). Then, tie rod length can be determined as: $t_r = |\overrightarrow{EF}|$, and effective steering arm length (ED) can be calculated by using the point to line distance formula as: $s_a = |\overrightarrow{EA} \times \overrightarrow{EB}|/|\overrightarrow{BA}|$.

Toe variation of the mechanism due to input θ can be determined by focusing the constraints in *OADEFO* loop. The first constraint states that for every position of the mechanism tie rod length remains constant, thus:

$$t_r{}^2 = (E_x - F_{x0})^2 + (E_y - F_{y0})^2 + (E_z - F_{z0})^2 \tag{7}$$

The second constraint states that for every position of the mechanism steering arm length remains constant, thus:

$$s_a{}^2 = (D_x - E_x)^2 + (D_y - E_y)^2 + (D_z - E_z)^2 \tag{8}$$

where

$$\overrightarrow{D} = l_l\overrightarrow{e_l} + l_a\overrightarrow{e_k} \quad , \quad l_a = \sqrt{|\overrightarrow{AE}|^2 - s_a^2}$$

The third constraint states that for every position of the mechanism the steering arm vector and the knuckle vector are perpendicular to each other ($\overrightarrow{ED} \perp \overrightarrow{AD}$). Since scalar product of two perpendicular vectors is equal to zero; $\overrightarrow{ED} \cdot \overrightarrow{AD} = 0$.

$$\left(l_l\overrightarrow{e_l} + l_a\overrightarrow{e_k} - (E_x\vec{i} + E_y\vec{j} + E_z\vec{k})\right) \cdot (l_a\overrightarrow{e_k}) = 0 \tag{9}$$

Rearranging Eq. (9) we obtain:

$$c_1E_x + c_2E_y + c_3E_z + c_4 = 0 \tag{10}$$

where the known parameters are:

$$c_1 = -l_a\overrightarrow{e_{kx}}, \quad c_2 = -l_a\overrightarrow{e_{ky}}, \quad c_3 = -l_a\overrightarrow{e_{kz}}, \quad c_4 = l_a{}^2 + l_l l_a(\overrightarrow{e_{kx}}\overrightarrow{e_{lx}} + \overrightarrow{e_{ky}}\overrightarrow{e_{ly}} + \overrightarrow{e_{kz}}\overrightarrow{e_{lz}})$$

In Eqns. (7), (8), and (10) the unknown parameters are E_x, E_y, and E_z which are the new coordinates of the spherical joint E of the steering arm. These three equations can be solved for three unknowns. At this stage, all positions of the joints are determined.

Now formulations for camber, caster, kingpin, toe angles, and track variation with respect to wheel travel are required to complete the analysis. Generally in suspension analyses, variation of these parameters with respect to wheel travel is preferred. Although we specified the lower wishbone angle as input variable, corresponding wheel travel is calculated for demonstration purpose. In order to determine wheel travel accurately, vectors through the point of contact of tire to the wheel hub should be calculated. Therefore, vectors between the points *HG*, *GW*, and *WJ* are required (Fig. 2). In this study, "static position" of the suspension system presents the position where both wheel travel and steering angle is equal to zero. The static position is presented by subscript "$_0$". At static position, rotation axis of the hub must be on XZ plane. Thus, at the static position of the suspension system, unit vector of the hub (GW) can be determined as:

$$\overrightarrow{e_{hub_0}} = [\cos\varepsilon_0 \quad 0 \quad -\sin\varepsilon_0]^T \tag{11}$$

where ε_0 is the positive static camber position of wheel (Fig. 3(a)). The static position of wheel center can be determined from:

$$\overrightarrow{l_{hubt_0}} = c_0[0 \quad -1 \quad 0]^T + l_{hub}\overrightarrow{e_{hub_0}} \tag{12}$$

[DOI: 10.1299/jamdsm.2015jamdsm0037]

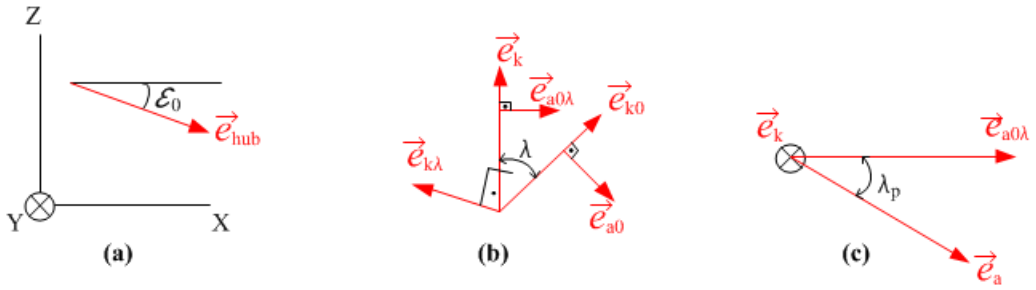

Fig. 3. Vector transformations

In order to obtain any position of the vectors which are on the knuckle, rotation matrices can be used and the following procedure can be employed. Caster offset *GH*, hub *GW*, and steering arm *ED* are on the same rigid body (parts of the knuckle) thus, all of the unit vectors on this body will have the same rotation during motion of the suspension. Therefore, once rotation of any unit vector is determined (e.g $\overrightarrow{e_a}$), other unit vectors can be determined with the associated rotation matrices. Now, let's determine rotation matrices of the unit vector of steering arm from its initial position (static position) $\overrightarrow{e_{a_0}}$ to any position $\overrightarrow{e_a}$. Here, rotation of the knuckle is considered to be superposition of two different rotations. Initially, rotation of the knuckle about its own axis is disregarded. Since the unit vector $\overrightarrow{e_k}$ is calculated from Eq. (5) for every position of the mechanism (for every θ), the amount of rotation of $\overrightarrow{e_k}$ can be determined from cross product as:

$$\lambda = \sin^{-1}\left[\left(\overrightarrow{e_{k_0}} \times \overrightarrow{e_k}\right) \cdot \overrightarrow{e_{k\lambda}}\right] \tag{13}$$

where $\overrightarrow{e_{k\lambda}}$ is the rotation axis which is perpendicular to the plane constituted by $\overrightarrow{e_k}$ and $\overrightarrow{e_{k_0}}$ as seen in Fig. 3(b), and it is determined as:

$$\overrightarrow{e_{k\lambda}} = \left(\overrightarrow{e_{k_0}} \times \overrightarrow{e_k}\right) / \left|\overrightarrow{e_{k_0}} \times \overrightarrow{e_k}\right|$$

Since, $\overrightarrow{e_a}$ is fixed on $\overrightarrow{e_k}$, after obtaining the amount of rotation λ, $\overrightarrow{e_{a0\lambda}}$ is also determined as seen in Fig. 3(b).

The second rotation required to complete the analysis is the rotation of knuckle about the unit vector $\overrightarrow{e_k}$, which can be determined from Fig. 3(c) as:

$$\lambda_p = \sin^{-1}\left[\left(\overrightarrow{e_{a0\lambda}} \times \overrightarrow{e_a}\right) \cdot \overrightarrow{e_k}\right] \tag{14}$$

The rotation matrix about an axis in the direction of unit vector $\vec{u}$, by an angle of θ is:

$$R(\vec{u},\theta) = \begin{bmatrix} \cos\theta + u_x^2(1-\cos\theta) & u_x u_y(1-\cos\theta) - u_z\sin\theta & u_x u_z(1-\cos\theta) + u_y\sin\theta \\ u_y u_x(1-\cos\theta) + u_z\sin\theta & \cos\theta + u_y^2(1-\cos\theta) & u_y u_z(1-\cos\theta) - u_x\sin\theta \\ u_z u_x(1-\cos\theta) - u_y\sin\theta & u_z u_y(1-\cos\theta) + u_x\sin\theta & \cos\theta + u_z^2(1-\cos\theta) \end{bmatrix}$$

Since we obtained the associated rotation matrices, the unit vector $\overrightarrow{e_{hub}}$ from its initial position ($\overrightarrow{e_{hub0}}$) to any current position can be determined as:

$$\overrightarrow{e_{hub}} = R(\overrightarrow{e_k}, \lambda_p)\, R(\overrightarrow{e_{k\lambda}}, \lambda)\, \overrightarrow{e_{hub_0}} \tag{15}$$

Similarly, using the same rotation matrices any position of the wheel hub can be determined as:

$$\overrightarrow{e_{hubt}} = R(\overrightarrow{e_k}, \lambda_p) R(\overrightarrow{e_{k\lambda}}, \lambda) \overrightarrow{e_{hubt_0}} \tag{16}$$

[DOI: 10.1299/jamdsm.2015jamdsm0037]

Thus, $\overrightarrow{l_{\mathrm{hubt}}} = \overrightarrow{e_{\mathrm{hubt}}} l_{\mathrm{hubt}}$

The last step is to determine the vector between the points *WJ*. The unit vector of this line $\overrightarrow{e_{\mathrm{tr}}}$ must be on XZ plane, since it is the shortest distance between point *W* and tire contact at ground *J*. Thus, $\overrightarrow{e_{\mathrm{tr}}} = [t_{\mathrm{rx}} \quad 0 \quad t_{\mathrm{rz}}]^T$.

Note that, ${t_{\mathrm{rx}}}^2 + {t_{\mathrm{rz}}}^2 = 1$.

Also note that, $\overrightarrow{e_{\mathrm{tr}}}$ must be perpendicular to $\overrightarrow{e_{\mathrm{hub}}}$, because $\overrightarrow{e_{\mathrm{hub}}}$ represents the direction of wheel rotation. Therefore, dot product of these vectors is equal to zero: $e_{\mathrm{hubx}} \cdot t_{\mathrm{rx}} + e_{\mathrm{hubz}} \cdot t_{\mathrm{rz}} = 0$

According to these conditions $\overrightarrow{e_{\mathrm{tr}}}$ can be determined as:

$$\overrightarrow{e_{\mathrm{tr}}} = \left[\mp \frac{e_{\mathrm{hubz}}}{e_{\mathrm{hubx}}} \sqrt{\frac{1}{\left(\frac{e_{\mathrm{hubz}}}{e_{\mathrm{hubx}}}\right)^2 + 1}} \qquad 0 \qquad \pm \sqrt{\frac{1}{\left(\frac{e_{\mathrm{hubz}}}{e_{\mathrm{hubx}}}\right)^2 + 1}} \right]^T \tag{17}$$

Wheel travel can be determined from the difference between initial and current positions of the vector from point *O* to *J*: $\overrightarrow{\Delta OJ} = \overrightarrow{OJ} - \overrightarrow{OJ_0}$

Thus, it can be determined by using Eqns. (5), (6), (16), and (17) as:

$$\overrightarrow{\Delta OJ} = \left(l_{\mathrm{l}}\overrightarrow{e_{\mathrm{l}}} + l_{\mathrm{h}}\overrightarrow{e_{\mathrm{k}}} + \overrightarrow{l_{\mathrm{hubt}}} + R_{\mathrm{w}}\overrightarrow{e_{\mathrm{tr}}}\right) - \left(l_{\mathrm{l}}\overrightarrow{e_{\mathrm{l}_0}} + l_{\mathrm{h}}\overrightarrow{e_{\mathrm{k}_0}} + \overrightarrow{l_{\mathrm{hubt}_0}} + R_{\mathrm{w}}\overrightarrow{e_{\mathrm{tr}_0}}\right) \tag{18}$$

Z-component of the vector given in Eq. (18), ΔOJ_{z} is the wheel travel of the suspension. From X-component of this vector the track variation can be determined as $2\Delta OJ_{\mathrm{x}}$. Here, ΔOJ_{x} is multiplied by two, since the track variation is calculated for two wheels.

Finally, camber, caster, kingpin, and toe angles are measured as shown in Fig. 4. Camber angle of the suspension system regarding the toe angle variation can be calculated from the angle between the hub direction and Z-axis as:

$$\varphi = \cos^{-1}(\overrightarrow{e_{\mathrm{hub}}} \cdot \vec{k}) - \pi/2 \tag{19}$$

Caster angle of the suspension system regarding the toe angle variation can be calculated from the angle between the unit vector perpendicular to the projection of the hub direction on XY plane and the unit vector of the knuckle as:

$$\tau = \cos^{-1}(\overrightarrow{e_{\mathrm{k}}} \cdot \overrightarrow{e_{\mathrm{caster}}}) - \pi/2 \tag{20}$$

where

$$\overrightarrow{e_{\mathrm{caster}}} = \left[\mp \frac{e_{\mathrm{huby}}}{e_{\mathrm{hubx}}} \sqrt{\frac{1}{\left(\frac{e_{\mathrm{huby}}}{e_{\mathrm{hubx}}}\right)^2 + 1}} \qquad \pm \sqrt{\frac{1}{\left(\frac{e_{\mathrm{huby}}}{e_{\mathrm{hubx}}}\right)^2 + 1}} \qquad 0 \right]^T$$

Kingpin angle of the suspension system regarding the toe angle variation can be calculated from the angle between the projection of the hub direction on XY plane and the unit vector of the knuckle as:

$$\sigma = \cos^{-1}(\overrightarrow{e_{\mathrm{k}}} \cdot \overrightarrow{e_{\mathrm{hubp}}}) - \pi/2 \tag{21}$$

where

$$\overrightarrow{e_{\mathrm{hubp}}} = \left[e_{\mathrm{hubp_x}} \quad e_{\mathrm{hubp_y}} \quad 0\right]^T / \sqrt{{e_{\mathrm{hubp_x}}}^2 + {e_{\mathrm{hubp_y}}}^2}$$

Toe angle of the suspension system can be determined from the angle between the projection of the hub direction on XY plane and Y-axis as:

[DOI: 10.1299/jamdsm.2015jamdsm0037]

$$\beta = \pi/2 - \cos^{-1}\left(\overrightarrow{e_{\text{hubp}}} \cdot \vec{j}\right) \tag{22}$$

where positive values of β represents toe-in and negative values represents toe-out.

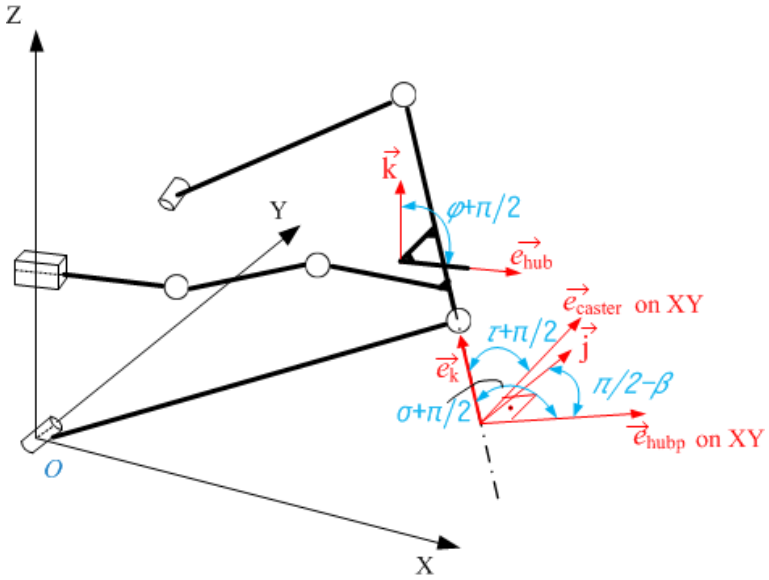

Fig 4. Camber, caster, kingpin, and toe angle measurement

4. Example

Analyze a double wishbone suspension mechanism for the following parameters: l_l = 330mm, l_u = 260mm, l_k = 240mm, p = 210mm, g = 32mm, f = -12mm, l_h = 120mm, c_o = 0, l_{hub} = 60mm, E_0 = [260 -120 173]^T, F_0 = [16 -59 150]^T, ϕ = 9°, ξ = 0, and ε_0 = -0.25°. The wheel travel is ±58mm, where positive values represents bump and negative values represents rebound respectively. Effective radius of the tire is R_w = 305mm.

Let the lower wishbone working range is: -10°≤ θ ≤10°. If Eqns. (4)-(18) are solved accordingly, the wheel travel is obtained as: -57.8mm≤ΔOJ_z ≤58.1mm. From Eqns. (19) and (20) camber angle and caster angle variations with respect to wheel travel can be determined as in Fig. 5.

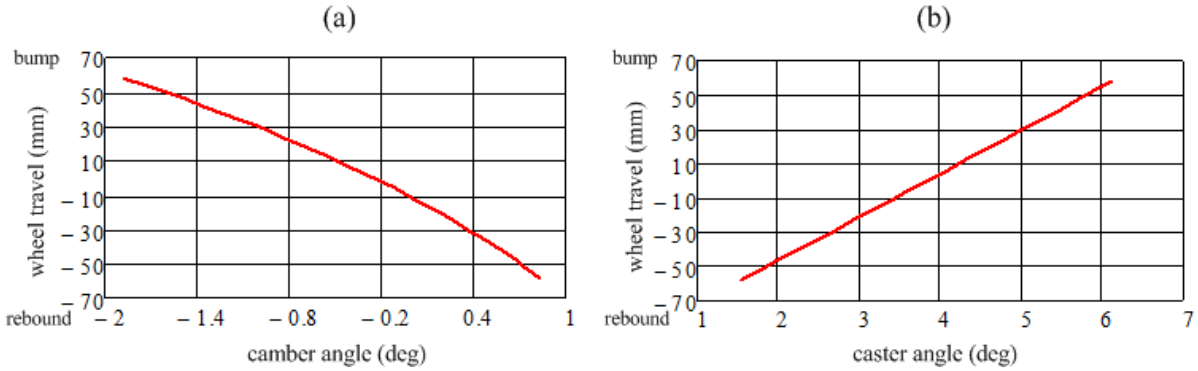

Fig. 5. Camber (a) and caster (b) angle w.r.t wheel travel

From Fig. 5(a) it can be observed that, static camber value that corresponds to zero wheel travel is equal to -0.25°, and the camber angle varies between -1.9°…+0.83° throughout the wheel travel. From Fig. 5(b), static caster angle value of the suspension system is observed as 3.9°, and the caster angle varies between 1.5°…6.1° throughout the wheel travel.

From Eqns. (21) and (22) kingpin and toe angle variations with respect wheel travel can be determined as in Fig. 6. As it is observed from Fig. 6(a), static kingpin value is equal to 9.4°, and kingpin angle varies between 8.4°…11.1°

[DOI: 10.1299/jamdsm.2015jamdsm0037]

throughout the wheel travel. From Fig. 6(b) it is observed that, static toe angle is equal to zero, and max toe angle value during a bump is equal to -0.9°. From Eq. (18) the track variation with respect to wheel travel can be determined as in Fig. 7.

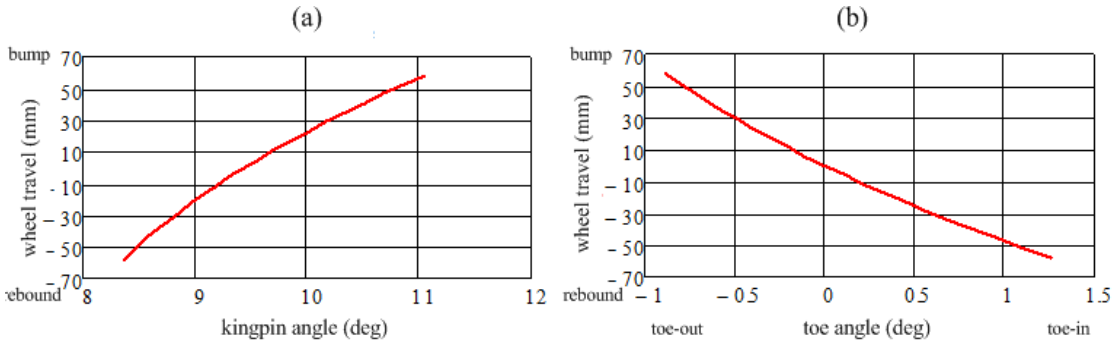

Fig. 6. Kingpin (a) and toe (b) angle w.r.t wheel travel

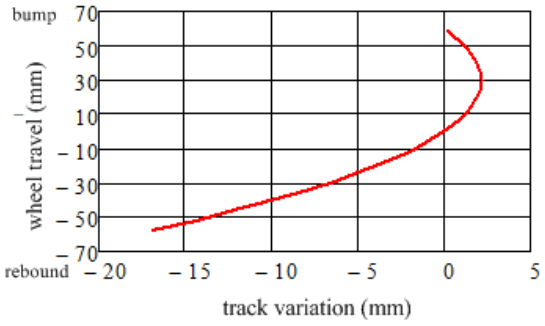

Fig. 7. Track variation w.r.t wheel travel

The results which are determined by the analytical model proposed in this study should be verified by other means. For this purpose, two different verification tools are employed. The same double wishbone suspension mechanism is modeled both in Catia and Lotus Suspension Analysis. The values of camber, caster, kingpin, and toe angles are checked accordingly. Since the analyzed system is a rigid mechanism the results should be same (or extremely small). As expected, the same results with the analytical model are obtained both in Catia and Lotus. In Table 1, a comparison chart is displayed for five different wheel travel values. Here, *A* represents the analytical model, *C* represents Catia and *L* represents Lotus. The small differences for caster and kingpin values at Lotus software results are due to interpolation errors; the Lotus software cannot show the result for corresponding wheel travel thus, we made interpolation from neighboring results.

Table 1. Comparison chart

Wheel	Camber (°)			Caster (°)			Kingpin (°)			Toe (°)		
Tra.(mm)	*A*	*C*	*L*	*A*	*C*	*L*	*A*	*C*	*L*	*A*	*C*	*L*
58.1	-1.88	-1.88	-1.88	6.13	6.13	6.10	11.1	11.1	11.2	-0.89	-0.89	-0.89
29.1	-0.99	-0.99	-0.99	5	5	5	10.2	10.2	10.2	-0.49	-0.49	-0.49
0	-0.25	-0.25	-0.25	3.86	3.86	3.89	9.44	9.44	9.46	0	0	0
-29	0.35	0.35	0.35	2.71	2.71	2.74	8.84	8.84	8.82	0.58	0.58	0.58
-57.8	0.83	0.83	0.83	1.55	1.55	1.58	8.36	8.36	8.33	1.26	1.26	1.26

[DOI: 10.1299/jamdsm.2015jamdsm0037]

5. Conclusions

In this study, initially kinematic model of the double wishbone mechanism is established. Then, an analysis procedure of the double wishbone mechanism is presented. For verification purpose, two different software packages are utilized and it is observed that results of the analytical model are same with the results of commercial software. Thus, it is verified that the proposed analytical model can be used precisely for the kinematic analysis and design of double wishbone mechanism instead of commercial software.

During analysis with commercial software packages, suspensions must be re-drawn each time when dimensions, orientations, and hard points are changed. However, with this analytical approach only the input variables of the code are changed and camber, caster, kingpin (steering axis inclination), toe, and track variation with respect to wheel travel are displayed instantly. Mechanisms of different dimensions can be analyzed and parameters can be optimized swiftly. Thus, time consumed during design stage decreases significantly by the aid of this analytical approach.

References

Attia, H.A., Dynamic modelling of the double wishbone motor-vehicle suspension system, Europ. J. of Mechanics A/Solids, Vol. 21 (2002), pp. 167-174.

Bae, S., Lee, J.M. and Chu, C.N., Axiomatic design of automotive suspension systems, CIRP Annals-Manufacturing Technology, Vol. 51 (2002), pp. 115-118.

Balike, K.P., Rakheja, S. and Stiharu, I., Development of kineto-dynamic quarter-car model for synthesis of a double wishbone suspension, Veh. Syst. Dyn., Vol. 49 (2011), pp. 107–128.

Habibi, H., Shirazi, K.H. and Shishesaz, M., Roll steer minimization of McPherson-strut suspension system using genetic algorithm method, Mechanism and Machine Theory, Vol. 43, No. 1 (2008), pp. 57-67.

Raghavan, M., An atlas of linkages for independent suspensions, SAE Papers, 911925 (1991).

Reimpell, J. and Stoll, H., The automotive chassis: engineering principles (1998), Vogel-Buchverlag, Würzburg.

Russell, K., Shen, Q., Lee, W.T. and Sodhi, R. S., On the Synthesis of Spatial RRSS Motion Generators with Prescribed Coupler Loads, Journal of Advanced Mechanical Design, Systems, and Manufacturing, Vol. 3, No. 3 (2009), pp. 236-244.

Sancibrian, R., Garcia, P., Viadero, F., Fernandez, A. and De-Juan, A., Kinematic design of double-wishbone suspension systems using a multiobjective optimisation approach, Veh. Syst. Dyn., Vol. 48 (2010), pp. 793–813.

Shen, Q., Lee, W.T and Russell, K., A small-scale optimization model for RSSR-SS motion generation with branch and order defect elimination in Matlab, Journal of Advanced Mechanical Design, Systems, and Manufacturing, Vol.8, No. 3 (2014), pp. 1-8.

Suh, C.H., Synthesis and analysis of suspension mechanisms with use of displacement matrices, SAE Papers, 890098 (1989), pp.189–200.

Tanık, E. and Parlaktas, V., A new type of compliant spatial four-bar (RSSR) mechanism, Mechanism and Machine Theory, Vol. 46 (2011), pp. 593–606.

Tanık, E. and Parlaktas, V., Design of a very light L7e electric vehicle prototype, International Journal of Automotive Technology, Vol. 16, No. 6 (2015), pp. 997–1005.

Tanık, E. and Parlaktas, V., Fully compliant spatial four-bar mechanism, Journal of Advanced Mechanical Design, Systems, and Manufacturing, Vol. 9, No. 1 (2015), pp. 1-12.

Uberti, S., Gadola, M., Chindamo, D., Romano, M. and Galli, F., Design of a double wishbone front suspension for an orchard–vineyard tractor: Kinematic analysis, J. of Terramechanics, Vol. 57 (2015), pp. 23–39.

Wu, J., Luo, Z., Zhang, Y. and Zhang, N., An interval uncertain optimization method for vehicle suspensions using Chebyshev metamodels, App. Math. Model, Vol. 38 (2014), pp. 3706–3723.

[DOI: 10.1299/jamdsm.2015jamdsm0037]